$SrCl_2$. Part of the greater linewidth in the CaF_2 at 4.2°K is due to unresolved fluorine hyperfine structure. This structure is temperature-dependent and was resolved by Bessent and Hayes[20] for Tm^{2+}, and Ranon and Hyde[21] in Yb^{3+} in the region between 4.2 and 20°K.

The production of Tm^{2+} in CaO is the first reduction of a rare earth in a cubic crystal with sixfold coordination or in a crystal in which the anion is not a halide. The observed production of Tm^{2+} in sites of cubic symmetry only is in line with previous work on the alkaline-earth halides. The sensitivity of the divalent Tm in CaO to thermal bleaching is unusual and indicates the irradiation-produced hole is more mobile at low temperatures than is the case in the alkaline-earth halides.

[20] R. G. Bessent and W. Hayes, Proc. Roy. Soc. (London) **A285**, 430 (1965).
[21] U. Ranon and James S. Hyde, Phys. Rev. **141**, 259 (1966).

ACKNOWLEDGMENTS

The authors wish to acknowledge the assistance of E. G. Clardy in growing the crystals, W. A. Sibley for the electron irradiations, and J. L. Kolopus for helpful discussions.

PHYSICAL REVIEW VOLUME 175, NUMBER 2 10 NOVEMBER 1968

Analysis of the Ground Term of Triply Ionized Terbium in Calcium Tungstate

D. E. WORTMAN

Harry Diamond Laboratories, Washington, D. C.

(Received 1 July 1968)

The energy levels of the ^7F ground term of Tb^{3+} in single crystals of $CaWO_4$ were established by absorption and fluorescence spectrum measurements. The measurements were made using crystals at temperatures between about 4.2 and 77°K. A study was made to determine the effects of the crystalline host material on these Tb^{3+} energy levels and to compare five theoretical models which can be used to describe such effects. The comparison of these Hamiltonians, using an effective Hamiltonian for the ground term suggested by Karayianis as the standard, shows that J mixing and term mixing significantly change the crystal-field parameters, and indicates to some extent the range of validity of these parameters. A least-squares fit was made between the experimental energy levels and the calculated ones for the ground term in each case. In one case, for example, where the effective Hamiltonian was used, the states of the ground term were described by Russell-Saunders wave functions. The calculation of the energy levels in this case takes into account the complete J mixing of the states within the ground term, and is equivalent to determining the effects of the spin-orbit interaction to second order. Use of this effective Hamiltonian yields a least-squares rms deviation of 60 cm^{-1} between the theoretical and experimental energy levels. The parameters of this effective Hamiltonian $H=\lambda_1(\mathbf{L}\cdot\mathbf{S})+\lambda_2(\lambda_1)(\mathbf{L}\cdot\mathbf{S})^2+\Sigma_{lm}B^{\dagger}_{lm}C_{lm}$ which yielded this fit, in cm^{-1}, are as follows: $\lambda_1=-272.7$, $\lambda_2(\lambda_1)=-4.837$, $B_{20}=466.1$, $B_{40}=-931.4$, $B_{44}=1032.4$, $B_{60}=-182.6$, $\mathrm{Re}B_{64}=571.6$, and $\mathrm{Im}B_{64}=0.023$. Parameters determined similarly using four other Hamiltonians show how sensitive the B_{lm} are to the choice of model. The $g_{\parallel}$ factor for the ground state of Tb^{3+} in $CaWO_4$ predicted by using each Hamiltonian is in agreement, to about 1.2%, with the experimental value $g_{\parallel}=17.777\pm0.005$ determined by Forrester and Hempstead in a previous EPR study.

I. INTRODUCTION

A STUDY has been made of the absorption and fluorescence spectra of Tb^{3+} in single crystals of $CaWO_4$ for the purpose of establishing the energy levels of the ^7F ground term of Tb^{3+} and determining the effects of the crystalline host material on these energy levels. The study also includes a comparison of various theoretical models which have been used to describe such effects. The effect of the host material on the Tb^{3+} energy levels is introduced in the calculations by the following Hamiltonian:

$$H_x=\sum_e\sum_{lm}B_{lm}{}^{\dagger}C_{lm}(\hat{r}_e), \tag{1}$$

where the e summation is over the electrons of the terbium ion. Here the C_{lm} are spherical tensors that are given in terms of the spherical harmonics Y_{lm} as follows:

$$C_{lm}=[4\pi/(2l+1)]^{1/2}Y_{lm}, \tag{2}$$

and the B_{lm} are defined by

$$B_{lm}=A_{lm}r^l. \tag{3}$$

The A_{lm} are the crystal-field parameters which represent the effect of the host-crystal structure, and it is assumed that the equivalent electron picture is valid. In this context, the expectation value of the electron's radial distance from the origin, $\langle r^l\rangle$, which enters the calculations is a function only of the impurity ion.

A determination of the A_{lm} for $CaWO_4$ is of particular interest, since this material has been used successfully as a laser material when doped with other rare-earth impurity ions such as Nd^{3+}. An accurate description of

the A_{lm} is needed to make calculations concerning many of the physical phenomena associated with laser action such as lifetimes, frequencies, and intensities. The crystal-field parameters are also important in that they can be used in studies to determine more about the crystal structure itself. For example, A_{lm} determined from lattice sum calculations based on point charges can be compared with those reported here, which were determined empirically by fitting calculated energy levels to the experimental levels. Such comparisons may aid in determining how the impurity ion acts to distort the host crystal structure, how the charge distribution differs from point charges, or how shielding and covalency effects enter in.

Before meaningful empirical values for the B_{lm} or A_{lm} can be determined, an adequate theoretical model that describes the free-ion energy levels must be found. Any inadequacies in describing the free-ion levels will manifest themselves in the crystal-field parameters. For this reason, one purpose of this work is to study five Hamiltonians listed below to determine to what degree the B_{lm} are sensitive to various theories. Thus, the detailed spectrum of the ground term of Tb^{3+} is used to show generally how various approximations affect the crystal-field parameters obtained empirically. The five Hamiltonians studied are the following.

Case 1:

$$H=H_x, \qquad \text{given by Eq. (1)} \tag{4}$$

Case 2:

$$H=\lambda(\mathbf{L}\cdot\mathbf{S})+H_x, \tag{5}$$

Case 3:

$$H=\lambda_1(\mathbf{L}\cdot\mathbf{S})+\lambda_2(\lambda_1)(\mathbf{L}\cdot\mathbf{S})^2+H_x, \tag{6}$$

where λ_1 and $\lambda_2(\lambda_1)$ are defined in Eq. (10),

Case 4:

$$H=\lambda_1(\mathbf{L}\cdot\mathbf{S})+\lambda_2(\mathbf{L}\cdot\mathbf{S})^2+H_x, \tag{7}$$

where λ_1 and λ_2 are independent parameters,

Case 5:

$$H=\lambda_1(\mathbf{L}\cdot\mathbf{S})+\lambda_2(\mathbf{L}\cdot\mathbf{S})^2+\lambda_3(\mathbf{L}\cdot\mathbf{S})^3+H_x, \tag{8}$$

where λ_1, λ_2, and λ_3 are independent parameters.

Equations (4)–(8) will be referred to in this paper as cases 1–5, respectively.

The Hamiltonian given by Eq. (4), case 1, neglects J mixing and term mixing; case 2 neglects term mixing, but allows for J mixing of the ground-term energy levels. Case 3, which was suggested[1] recently and which will be used as the standard for comparison purposes in this work, includes both of these effects and yet does not introduce any additional free parameters into the calculations. A recent study[1] shows that for the ground term an effective spin-orbit Hamiltonian can be used which relates λ_1 and λ_2 (case 3) as follows:

$$H_{so}=\lambda_1(\mathbf{L}\cdot\mathbf{S})+\lambda_2(\mathbf{L}\cdot\mathbf{S})^2, \tag{9}$$

where

$$\lambda_1=F_2\eta(1+a\eta), \qquad \lambda_2=F_2\eta^2 b, \tag{10}$$

and

$$\eta=\epsilon\zeta/2SF_2. \tag{11}$$

Here a and b represent the contribution from second-order effects of the spin-orbit interaction, F_2 is the usual[2] Slater parameter, ζ is the expectation value of the spin-orbit coupling constant[3] $\langle\xi\rangle$, and S is the total spin of the ground term. In Eq. (11), $\epsilon=+1$ if the number of equivalent electrons is $\leq 2l+1$ (half-shell), and $\epsilon=-1$ if the number of equivalent electrons is $>2l+1$. Also the calculation using case 3 has been shown[1] to be equivalent to determining the effects of the spin-orbit interaction to second order, and by diagonalizing this effective Hamiltonian in the states described in the ground term, full J mixing of the states by the crystal field is allowed. In case 4, by allowing λ_1 and λ_2 to vary freely, one can determine to some degree how uncertainties in F_2, a, and b affect the B_{lm}. In case 5, by introducing a third parameter associated with $(\mathbf{L}\cdot\mathbf{S})^3$, the determination of similar effects by higher order spin-orbit terms can be made. At this time, one can not say which of these cases yields a better description of the system. However, for comparison purposes, case 3 is chosen as the standard model because λ_1 and λ_2 are related theoretically and one does not resort to a phenomenonlogical introduction of additional parameters as in cases 4 and 5.

Values for the parameters found for the five Hamiltonians mentioned above are given in Table IX. This table shows how the empirical B_{lm} change when higher-order effects are included in the calculations. These results indicate that the B_{lm} determined by neglecting J mixing and/or term mixing change significantly when such effects are considered. For example, B_{20} as determined in cases 1 and 2 are 446.7 and 486.1 cm^{-1}, respectively, whereas B_{20} determined in cases 3–5 are 466.1, 466.4, and 467.8 cm^{-1}, respectively. Thus B_{20} changes by about 9% when one uses case 1 instead of case 2; but it remains essentially the same, and about 5% from either the value of case 1 or case 2, for cases 3, 4, and 5. The variation in B_{40}, B_{44}, B_{60}, and $\mathrm{Re}B_{64}$ for cases 1–5 are 32, 26, 319, and 127%, respectively. The percentage variation in $\mathrm{Im}B_{64}$ is quite large, since it is near zero in every case except case 5; however, even here, the imaginary component is about $\frac{1}{4}$ the real component, which is consistent[4] with other work.

In determining the experimental energy levels, the absorption spectrum of Tb^{3+} in $CaWO_4$ was recorded over the wavelength range from 3000 to 26 000 A.

[1] N. Karayianis (to be published); Bull. Am. Phys. Soc. **13**, 686 (1968).

[2] B. R. Judd, *Operator Techniques in Atomic Spectroscopy* (McGraw-Hill Book Co., New York, 1963), p. 80.

[3] See, Ref. 2, p. 6.

[4] L. Y. Shekun, Opt. i Spektroskopyia **22**, 776 (1967) [English transl.: Opt. Spectry. (USSR) **22**, 422 (1967)].

Transitions from the ground $^7F_6$ multiplet to the J multiplets, 0, 1, 2, and 3 were observed in this wavelength range using crystals at temperatures between about 4.2 and 77°K. Emission from the $^5D_3$ and $^5D_4$ multiplets to the ^7F_J energy levels were observed in the wavelength range from 3750 to 7000 Å. The ^5D and higher-energy terms are relatively far above the ground ^7F term, which leads to a small admixture of higher-energy states with the ground term.

In determining the theoretical energy levels consistent with these measurements, the Hamiltonian of case 1 was diagonalized for each J multiplet of the ground term; the Hamiltonians of cases 2–5 were diagonalized in a basis of Russell-Saunders wave functions describing the states of the entire ^7F ground term. These theoretical energy levels were then compared with the observed energy levels, and a homing-in procedure was performed by an IBM-7094 computer which varied the B_{lm} and spin-orbit parameter(s) until a least-squares fit was obtained. The accuracies of these parameters is discussed in Sec. IV. The nonzero B_{lm} for S_4 symmetry, which were assumed in the calculations are B_{20}, B_{40}, B_{60}, B_{44}, ReB_{64}, and ImB_{64}, where in general B_{44} and B_{64} can be complex. However, one is free to choose a coordinate system in which representation B_{44} is real.

Values for A_{lm} were determined by interpolating from previous free-ion wave-function calculations[5] to obtain $\langle r^l \rangle$ of terbium. The values for the A_{lm} using the B_{lm} of case 3, are found to be as follows, in units of cm^{-1} × atomic units^{-l}:

$$A_{20}=352.4, \qquad A_{60}=-1039.4,$$
$$A_{40}=-1321.6, \qquad \mathrm{Re}A_{64}=3253.6,$$
$$A_{44}=1464.9, \qquad \mathrm{Im}A_{64}=0.131, \qquad (12)$$

where, in atomic units,

$$\langle r^2 \rangle=0.756, \quad \langle r^4 \rangle=1.419, \quad \langle r^6 \rangle=5.692. \quad (13)$$

These A_{lm} are limited both by the accuracy of the calculated $\langle r^l \rangle$ and by the validity of the interpolation, as well as by the accuracy of the empirical B_{lm}.

The theory and calculations are discussed in more detail in Sec. II. The experimental apparatus and procedure concerning both the absorption and fluorescence measurements are discussed in Sec. III. The experimental results and the results of the calculations are discussed in Sec. IV. The latter results indicate that J mixing and term mixing significantly affect the B_{lm}. The results also show that the effective Hamiltonian (case 3) is in better agreement with the measured energy splittings of the ground multiplets than levels predicted by the more commonly used Hamiltonians, cases 1 and 2. The significance of the results of cases 4 and 5 is discussed in Sec. IV. In addition, the $g_{||}$ factor of the ground state predicted by case 3 is 17.916, which is within 0.8% of the $g_{||}$ factor determined experimentally in a previous EPR study,[6] $g_{||}=17.777\pm0.005$. Though not in as good agreement as case 3, the $g_{||}$ factors found for cases 1, 2, 4, and 5 were found to be in agreement to within approximately 1.2% of the experimental value.

[5] A. J. Freeman and R. E. Watson, Phys. Rev. **127**, 2058 (1962).

II. THEORY AND CALCULATIONS

A. Theory

The ground term for the lowest energy configuration of Tb^{3+}, specified by eight $4f$ electrons, is ^7F. The ^7F_J energy states have been reported[7] as being more than 95% ^7F, and therefore it is expected that a pure Russell-Saunders calculation will give meaningful results. The wave functions are chosen such that the total orbital and spin angular momenta L and S and their z-axis projections M_L and M_S are good quantum numbers.

The trivalent terbium ion is assumed[6] to occupy the divalent calcium ion site in the crystal. The point symmetry at such a site is S_4. Each of the Russell-Saunders wave functions representing the eigenstates of the ^7F term of terbium have symmetry properties that can be classified according to one of four irreducible representations of the S_4 group which are designated Γ_1, Γ_2, Γ_3, and Γ_4. The symmetry properties yield that the crystal-field couples states where $\Delta M_L=0, \pm4$ and $\Delta M_S=0$ in addition to those coupled by the spin-orbit interaction which couples states where $\Delta M_J=0$ with $M_J=M_L+M_S$.

B. Calculations

The calculations will be described for case 3. Using this Hamiltonian one must compare the theoretical and experimental energy levels to obtain a best set of values for η and the B_{lm}. Values for F_2 as given by Ofelt,[7] and a and b as determined by Karayianis[1] which are used in these equations are

$$F_2=434 \text{ cm}^{-1},$$
$$a=3.3993\times10^{-2}, \text{ and } b=-2.7005\times10^{-2}. \quad (14)$$

To obtain the theoretical energy levels one diagonalizes a 37×37 matrix composed of Russell-Saunders states coupled by the Hamiltonian of case 3 (similarly for cases 2, 4, and 5). This breaks up into one 13×13 matrix of elements where states are coupled whose wave functions transform as the Γ_1 irreducible representation of the S_4 point symmetry group—designated a Γ_1 matrix—one 12×12 Γ_2 matrix, and one 12×12 $\Gamma_{3,4}$ matrix. The energy levels characterized by wave functions transforming as Γ_3 are degenerate with those transforming as Γ_4; hence they are designated $\Gamma_{3,4}$.

To determine the experimental levels with which the theoretical levels are to be compared, one makes use of

[6] P. A. Forrester and C. F. Hempstead, Phys. Rev. **126**, 923 (1962).

[7] G. S. Ofelt, J. Chem. Phys. **38**, 2171 (1963).

the symmetry properties at the terbium site. Calcium tungstate has three mutually perpendicular axes; two are equivalent (*a* axes) and one is unique (*c* axis). When light is propagated down an *a* axis of the crystal, the components of the electric and magnetic dipole operators parallel with the *c* axis transform as Γ_2 and Γ_1, respectively, and that component of these operators perpendicular to the *c* axis transforms as a $\Gamma_{3,4}$. When light is passed along the *c* axis, the electric and magnetic dipole operators transform as $\Gamma_{3,4}$. Using these properties of the crystal field at the Tb^{3+} site and the S_4 group multiplication tables,[8] an energy diagram may be made from the observed spectral lines.

III. EXPERIMENTAL PROCEDURE

A. Absorption Spectrum

The absorption spectrum of Tb^{3+} in single crystals of $CaWO_4$ was measured on a Cary-14 spectrophotometer over the wavelength range from 2.5 μ to the absorption edge at about 0.3 μ. The resolution of the instrument varies from about 3.0 Å (at 2.5 μ) to 1.0 Å (at 0.3 μ). Spectra were recorded with the crystal oriented such that light passed along the unique "*c* axis" of the crystal (axial spectrum) for one set of measurements, and such that it passed along one of the like "*a* axis" for the other measurements; i.e., unpolarized, π (electric vector parallel to *c* axis), and σ (electric vector perpendicular to *c* axis) spectra.

Single crystals grown (by the Czochralski method) from a melt containing between 0.25 and 1.5 at.% Tb^{3+} with 4:1 Na:Tb as charge compensator were used.[9] No extra lines were introduced by using the more heavily doped crystals. These crystals which were placed in contact with a copper cold-finger in a Dewar with thin quartz windows were generally run at temperatures near that of liquid helium (4.2°K) or of liquid nitrogen (77°K). Data were also recorded in warmup experiments with the crystal temperature approaching 300°K for the purpose of studying transitions originating from higher energy levels of the $^7F_6$ multiplet which are not (for all practical purposes) occupied at the lower temperatures.

B. Fluorescence Spectrum

The fluorescence lines were generally of low intensity. Therefore a 1.5% Tb^{3+}-doped single crystal of $CaWO_4$ (sodium-compensated) which yielded a relatively strong and sharp absorption spectrum was selected for the fluorescence measurements. This crystal was placed in a Dewar with thin quartz windows and was held in contact with a copper cold finger. Spectra were recorded with the crystal at temperatures near those of liquid helium and liquid nitrogen.

A 500-W Hg lamp was used as a light source in recording most of the data. Light from this source was passed through a quartz water cell to remove much of the ultraviolet and infrared radiation. This light was further filtered by a Corning No. 5874 filter (transmission through this filter peaks at a wavelength of about 0.365 μ, and cuts off at 0.3 and 0.41 μ). The light was then shined on the crystal mounted with its unique *c* axis aligned parallel with the slit of a $\frac{1}{2}$-m Jarrel Ash spectrometer. A photodetector with *S*-20 surface was used to detect the fluorescent light that was emitted perpendicular to the light beam which served to populate the higher energy levels of Tb^{3+}. The resolution of the instrument using a slit setting of 30 μ in this wavelength range was about 0.1% of the wavelength setting in A.

By the arrangement mentioned above, the $^5D_3$ and some higher energy levels were excited directly, but the $^5D_4$ energy levels were not. Transitions from these upper levels could then be observed to the $^5D_4$ and ^7F_J multiplets. Transitions could also be observed from the $^5D_4$ levels, which were now populated, to the ^7F_J levels. These transitions were the most useful owing to the fact that there is less background radiation and fewer fluorescing levels to complicate the region of interest. Transitions from the $^5D_3$ and higher energy levels substantiated the identification of the energy levels determined by the $^5D_4$-to-^7F_J transitions.

Polarizers were used to help in the analysis of the spectra. As a check to assure that none of the transitions observed were Hg lines, spectra were recorded using a 1-m Jarrell-Ash spectrometer and a 500-W neon lamp as the light source and the same experimental setup. The resolution of the instrument in this case was about the same as that obtained using the $\frac{1}{2}$-m Jarrell-Ash monochromator owing to the relatively low intensity of the fluorescence.

IV. RESULTS

A. Experimental Results

An energy level scheme shown in Figs. 1 and 2 was determined from the emission spectrum for the entire ground ^7F term of Tb^{3+} in $CaWO_4$ which is compatible with the energy levels determined from the absorption spectra measurements. The lowest-lying states of the ground $^7F_6$ multiplet were determined by previous EPR measurements[6] as being two Γ_2 states separated by approximately 0.27 cm^{-1}. These two energy levels could not be resolved in this work. Transitions from this optically degenerate Γ_2 ground state to the $^7F_0$, $^7F_1$, $^7F_2$, and $^7F_3$ multiplets were observed in absorption measurements using the crystal near liquid-helium temperature. Using the crystal at higher temperatures allowed transitions from two higher energy levels in the $^7F_6$ multiplet to be established. The transitions observed in these absorption data, some of which were

[8] G. F. Koster, J. O. Dimmock, R. G. Wheeler, and H. Statz, *Properties of the Thirty-Two Point Groups* (The MIT Press, Cambridge, Mass., 1963).

[9] K. Nassau, J. Phys. Chem. Solids, **24**, 1503 (1963).

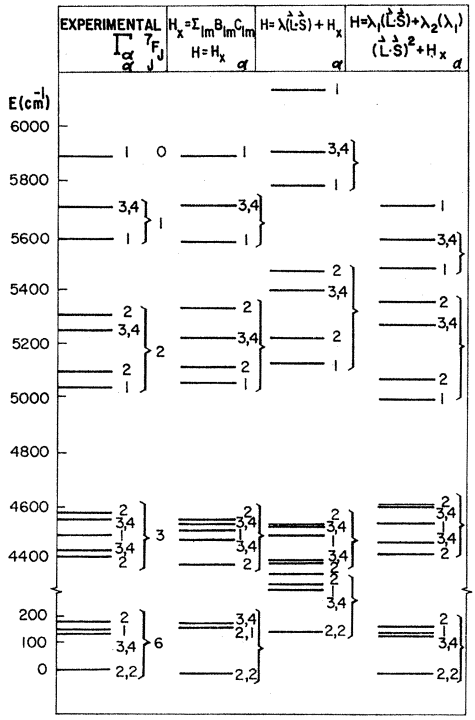

FIG. 1. Comparison of experimental and theoretical energy levels for the ground terms of Tb^{3+} in $CaWO_4$. Γ_α designates the symmetry of each ^7F_J state. These energy levels were recorded in both the absorption and fluorescence spectrum measurements.

published in an earlier report,[10] are shown in Fig. 1. These data were consistent with the electric-dipole operator selection rules but could not be explained by using the transformation properties of the magnetic dipole operator.

The emission lines corresponding to transitions from the $^5D_3$ and $^5D_4$ multiplets to the ^7F_J energy levels were recorded primarily to establish the remaining energy levels of the $^7F_4$, $^7F_5$, and $^7F_6$ multiplets. Absorption measurements were also taken in the region where one might expect transitions from the ground state to the $^5D_3$ and $^5D_4$ multiplets in the hope of identifying the fluorescing levels. Lines were observed at energies from 26 288 cm^{-1} upward corresponding to absorptions to the $^5D_3$ multiplet and from 20 542 cm^{-1} upward corresponding to transitions to the $^5D_4$ multiplet from the ground state. All the energy levels of these multiplets (discussed below in subsection 8) were not determined from these absorption data; hence a positive identification of the fluorescing levels could not be made. A consistent energy level scheme for Tb^{3+} in $CaWO_4$ could be made without a detailed knowledge of such multiplets, however, using the lines corresponding to transitions from the $^5D_4$ levels to the ^7F_J multiplets. The $^5D_3$ to ^7F_J lines were complicated by transitions from higher energy levels, as from the $^5L_{10}$, to lower-lying states; therefore such data were used only to substantiate the ^7F_J energy levels determined by the $^5D_4$ to ^7F_J transitions.

In the fluorescence data the highest-energy transition at 20 547 cm^{-1} was identified as being from the lowest-lying emitting level of the $^5D_4$ multiplet to the ground Γ_2 state. This value was subsequently used to construct the energy level scheme for the ground ^7F term of Tb^{3+} in $CaWO_4$ (Tables I–VII). In the Tables I–VII, columns A through D represent the fluorescence data. Column A is the identification made of the fluorescence line observed. Column B is a description of the line. Parentheses indicate the predominant polarization where the line is observed in both the σ and π spectra; S indicates an unresolved shoulder; Sl means a small line, b means the line is a small bump; and l designates a line. Generally, the lines were rather weak in intensity (compared with data recorded for Nd^{3+} or Yb^{3+} in $CaWO_4$) and varied in full width at half-maximum from about 10 to 50 cm^{-1}. Column C corresponds to the energy at the peak of the line, and column D represents the energy level of the state in Tb^{3+} obtained by subtracting column C from 20 547 cm^{-1} (the lowest fluorescing level of the $^5D_4$). Column E represents the energy levels established by the absorption measurements. Column F gives the experimental energy levels that were used in the calculations obtained by comparing the absorption and fluorescence energy levels.

The establishing of the energy level scheme given in

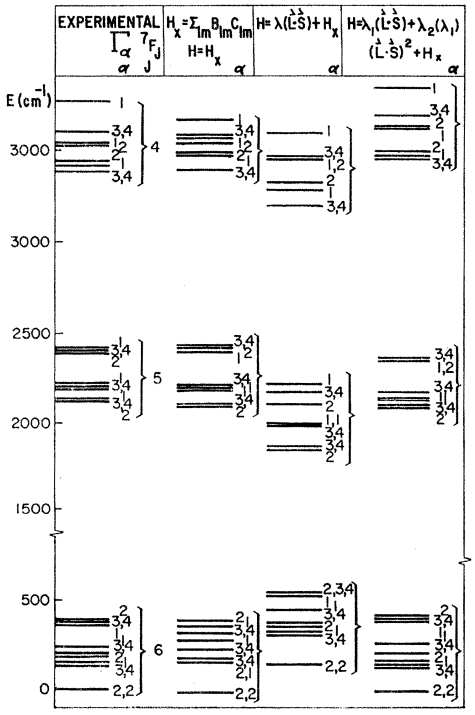

FIG. 2. Comparison of experimental and theoretical energy levels for the ground term of Tb^{3+} in $CaWO_4$. These energy levels were recorded in the fluorescence-spectrum measurements. Γ_α designates the symmetry of each ^7F_J state.

[10] D. E. Wortman, Harry Diamond Laboratory Report No. TR-1337, 1966 (unpublished).

TABLE I. Energy levels of $^7F_6$ multiplet of Tb^{3+} in $CaWO_4$. The fluorescence data described in columns A, B, and C are used to establish the $^7F_6$ energy levels shown in column D. Column E gives the $^7F_6$ energy levels established by absorption measurements. Columns F and G represent the experimental and theoretical energy levels used to obtain a best set of crystal-field parameters.

No.	A	B[a]	C	D	E	F	G
	$^5D_4$ to $^7F_6$ Γ_x	Description	Energy (cm^{-1})	20 547 cm^{-1} − C (cm^{-1})	Absorption levels (cm^{-1})	Experimental levels (cm^{-1})	Theoretical levels (cm^{-1})
1	Γ_2	l[π]	20 547	0	0	0	−7.61
2	Γ_2	l[π]	20 547	0	0.27	0.27	−6.87
3	($^5D_3 \rightarrow {}^7F_0$)	Sl[σ]	20 462				
4	$\Gamma_{3,4}$	l	20 412	135	135	135	130.2
5	Γ_1	Sσ	20 396	151		152	143.4
6	Γ_2	l[π]	20 371	176	180	180	166.4
7	$\Gamma_{3,4}$	lσ	20 346	201		202	198.6
8	Γ_1	lσ	20 313	234		235	257.9
9	Γ_1	Sσ	20 190	357		359	381.3
10	$\Gamma_{3,4}$	l[σ]	20 169	378		380	393.3
11	Γ_2	l[π]	20 161	386		388	400.2

[a] No polarization indicated means line observed about equally in σ and π. [ ] indicates dominant polarization when designation is uncertain. b = bump; l = line; Sl = small line; S = shoulder.

Tables I–VII for Tb^{3+} in $CaWO_4$ may be discussed best, perhaps, by considering each multiplet separately.

1. $^7F_6$ State

In the fluorescence data, ten lines were observed in the wavelength range where one might expect transitions from the $^5D_4$ to the $^7F_6$ multiplet (transitions to ten S_4 levels of the $^7F_6$ might be expected but two are known to be optically degenerate). These are listed in Table I. The small line observed at 4887 Å or 20 462 cm^{-1} was identified as being from the $^5D_3$ multiplet to the $^7F_0$ state, and this is consistent with the absorption data.

The polarizations of the recorded lines indicate the fluorescence may be originating from two very close energy levels in the $^5D_4$ multiplet, a $\Gamma_{3,4}$ and a Γ_1. From the S_4 group multiplication tables[8] and the transformation properties of the electric dipole operator (the component perpendicular to the c axis of the crystal transforms as a $\Gamma_{3,4}$ and the component parallel to the c axis transforms as a Γ_2), one might expect transitions from such $^5D_4$ levels to the Γ_2 and $\Gamma_{3,4}$ $^7F_6$ states to appear in both the σ- and the π-polarized spectra, and the transitions to the Γ_1 levels of the $^7F_6$ multiplet to be pure σ. This indeed seems to be the case for transitions from the $^5D_4$ to $^7F_6$ levels. This, likewise, is consistent with the absorption measurements, which indicated that the level at 20 542 cm^{-1} seen as a π line, is a $^7F_6$ Γ_2 to $^5D_4$ Γ_1 transition where the small σ component may be from the $^7F_6$ Γ_2 to a $^5D_4$ $\Gamma_{3,4}$.

2. $^7F_5$ State

Absorption lines were not observed to this $^7F_5$ multiplet. In fluorescence, ten lines were observed in the

TABLE II. Energy levels of $^7F_5$ multiplet of Tb^{3+} in $CaWO_4$. The fluorescence data described in columns A, B, and C are used to establish the $^7F_5$ energy levels shown in column D. No absorption lines were observed to this multiplet. Columns F and G represent the experimental and theoretical energy levels used to obtain a best set of crystal-field parameters.

No.	A	B	C	D	E	F	G
	$^5D_4$ to $^7F_5$ Γ_x	Description[a]	Energy (cm^{-1})	20 547 cm^{-1} − C (cm^{-1})	Absorption levels (cm^{-1})	Experimental levels (cm^{-1})	Theoretical levels (cm^{-1})
1	Γ_2	b	18 433	2114		2119	2092.9
2	$\Gamma_{3,4}$	b	18 416	2131		2136	2101.7
3	No. 6+50 cm^{-1}	l[π]	18 392				
4	No. 7+50 cm^{-1}	l	18 382				
5	Γ_1	l	18 365	2182		2188	2139.9
6	$\Gamma_{3,4}$	lπ	18 342	2205		2211	2173.1
7	Γ_1	lσ	18 332	2215		2221	2143.3
8	Γ_2	b[σ]	18 175	2372		2378	2355.4
9	$\Gamma_{3,4}$	l[π]	18 149	2398		2404	2363.4
10	Γ_1	l[σ]	18 139	2408		2414	2355.9

[a] Notation in column B, see Table I.

TABLE III. Energy levels of $^7F_4$ multiplet of Tb^{3+} in $CaWO_4$. The fluorescence data described in columns A, B, C are used to establish the $^7F_4$ energy levels shown in column D. No absorption lines were observed to this multiplet. Columns F and G represent the experimental and theoretical energy levels used to obtain a best set of crystal-field parameters.

No.	A	B	C	D	E	F	G
	$^5D_4$ to $^7F_4$ Γ_x	Description[a]	Energy (cm^{-1})	20 547 cm^{-1}—C (cm^{-1})	Absorption levels (cm^{-1})	Experimental levels (cm^{-1})	Theoretical levels (cm^{-1})
1	(No. 2+21 cm^{-1})	$Sl\pi$	17 194				
2	$\Gamma_{3,4}$	$l[\sigma]$	17 173	3374		3382	3458.7
3	(No. 7+53 cm^{-1})	S	17 165				
4		$S\pi$	17 144				
5	Γ_1	$l[\sigma]$	17 138	3409		3417	3478.4
6		b	17 123				
7	Γ_2	$l\pi$	17 112	3435		3443	3502.2
8	Γ_2	$l[\sigma]$	17 027	3520		3529	3638.4
9	Γ_1	$b\sigma$	17 015	3532		3541	3632.9
10	(No. 11+23 cm^{-1})	S	16 972				
11	$\Gamma_{3,4}$	$l[\sigma]$	16 949	3598		3607	3696.8
12	(No. 13+22 cm^{-1})	$l\pi$	16 801				
13	Γ_1	$l[\sigma]$	16 779	3768		3777	3851.6

[a] Notation in column B, see Table I.

wavelength range where one might expect transitions from the $^5D_4$ to the $^7F_5$ multiplet. According to the S_4 symmetry properties, the $^7F_5$ multiplet should consist of eight energy levels; i.e., three Γ_1's, two Γ_2's, and three $\Gamma_{3,4}$'s. Assuming that the lowest-lying levels of the $^5D_4$ multiplet which fluoresce to the $^7F_5$ multiplet are the two close energy levels, a Γ_1 and a $\Gamma_{3,4}$, as were consistent with the observations concerning the $^7F_6$ multiplet, one obtains the energy levels listed in Table II. A line at 18 392 cm^{-1} which is 50 cm^{-1} above one at 18 342 cm^{-1}, and a level at 18 382 cm^{-1} which is 50 cm^{-1} above one at 18 332 cm^{-1}, suggest that transitions originating at an upper level of the $^5D_4$ go to the same levels as do transitions from the lower fluorescing $^5D_4$ levels. The polarizations suggest that this upper fluorescing level in the $^5D_4$ multiplet is a Γ_2 at about 50 cm^{-1} above the lower Γ_1 and $\Gamma_{3,4}$ energy levels of the $^5D_4$. This could account for the two extra lines observed in the fluorescence data.

3. $^7F_4$ State

Transitions in the absorption spectra were not recorded from the ground state to the $^7F_4$ multiplet of Tb^{3+} in $CaWO_4$. Hence, again the fluorescence data had to be used to establish the energy levels. In the fluorescence spectra 13 lines were observed as shown in Table III. From these 13 lines, transitions to seven energy levels of the $^7F_4$ might be expected according to the S_4 symmetry predictions.

Three lines were observed at approximately 22 cm^{-1} above three other lines; i.e., 17 194 over 17 173 cm^{-1}, 16 972 over 16 949 cm^{-1}, and 16 801 over 16 779 cm^{-1}. Hence, another energy level approximately 22 cm^{-1} above the lower Γ_1 and $\Gamma_{3,4}$ levels of the $^5D_4$ multiplet may be fluorescing to at least three $^7F_4$ states. The polarizations of the transitions suggest that this fluorescing level is another $\Gamma_{3,4}$. A level at 17 165 cm^{-1} which is 53 cm^{-1} above the 17 112 cm^{-1} line is consistent as

TABLE IV. Energy levels of $^7F_3$ multiplet of Tb^{3+} in $CaWO_4$. The fluorescence data described in columns A, B, and C are used to establish the $^7F_3$ energy levels shown in column D. Column E gives the $^7F_3$ energy levels established by absorption measurements. Columns F and G represent the experimental and theoretical energy levels used to obtain a best set of crystal-field parameters.

No.	A	B	C	D	E	F	G
	$^5D_4$ to $^7F_3$ Γ_x	Description[a]	Energy (cm^{-1})	20 547 cm^{-1}—C (cm^{-1})	Absorption levels (cm^{-1})	Experimental levels (cm^{-1})	Theoretical levels (cm^{-1})
1	Γ_2	$l[\pi]$	16 124	4423	4419	4419	4428.9
2	$\Gamma_{3,4}$	$l[\sigma]$	16 113	4434	4444	4444	4473.2
3	Γ_1	$b\sigma$	16 062	4485	4499	4499	4543.5
4	$\Gamma_{3,4}$	$b[\pi]$	16 008	4539	4556	4556	4602.6
5	Γ_2	$b[\pi]$	15 974	4573	4580	4580	4605.4

[a] Notation in column B, see Table I.

TABLE V. Energy levels of $^7F_2$ multiplet of Tb^{3+} in $CaWO_4$. The fluorescence data described in columns A, B, and C are used to establish the $^7F_2$ energy levels shown in column D. Column E gives the $^7F_2$ energy levels observed in absorption measurements. Columns F and G represent the experimental and theoretical energy levels used to obtain a best set of crystal-field parameters.

No.	A	B	C	D	E	F	G
	$^5D_4$ to $^7F_2$ Γ_x	Description[a]	Energy (cm^{-1})	20 547 cm^{-1} − C (cm^{-1})	Absorption levels[b] (cm^{-1})	Experimental levels (cm^{-1})	Theoretical levels (cm^{-1})
1	Γ_1	bσ	15 523	5024	5039	5039	4999.8
2	Γ_2	l	15 468	5079	5098	5098	5070.1
3	$\Gamma_{3,4}$	l	15 314	5233	5247	5247	5269.6
4	Γ_2	S	15 253	5294	5308	5308	5355.4

[a] Notation in column B, see Table I. [b] Extra σ lines were seen in absorption at 5332, 5280, and 5263 cm^{-1}.

being from the upper Γ_2 state of the $^5D_4$ multiplet, which seemed to be fluorescing to the $^7F_5$ energy levels. Two other very low intensity "lines," a shoulder at 17 144 cm^{-1} on the 17 138-cm^{-1} line and a small bump at 17 123 cm^{-1}, were not accounted for. The other lines in the fluorescence data, which were much more pronounced, were regarded as corresponding to transitions from the lower Γ_1 and $\Gamma_{3,4}$ levels of the $^5D_4$ multiplet to the $^7F_4$ energy levels.

4. $^7F_3$ State

Three energy levels were established by the absorption data taken with the crystal at liquid-helium temperature (the two $\Gamma_{3,4}$'s and the Γ_1 level). The remaining two Γ_2 levels were obtained by warmup experiments in the absorption work.

Transitions were observed in the fluorescence data corresponding to transitions from the lower $^5D_4$ fluorescing levels to all the $^7F_3$ states. These data and their interpretations are given in Table IV.

5. $^7F_2$ State

Again the energy levels were established by both the absorption and fluorescence measurements and these are given in Table V. Extra lines were seen in the absorption spectra in the energy region near the $\Gamma_{3,4}$ level. In an earlier report,[11] the $\Gamma_{3,4}$ level was identified as having an energy of 5247 cm^{-1}. The fluorescence data are consistent with this assignment.

6. $^7F_1$ State

Two energy levels were observed in the absorption data, a π line at 5585 cm^{-1} (identified as the Γ_1 level) and a σ line at 5702 cm^{-1} (the $\Gamma_{3,4}$ level). Two lines were also seen in the fluorescence data, a σ line at 14 975 cm^{-1} and a π line at 14 852 cm^{-1}. These would be consistent as being transitions from the $\Gamma_{3,4}$ level of the $^5D_4$ multiplet. These data are given in Table VI.

7. $^7F_0$ State

One π line was seen in the absorption spectrum at 5890 cm^{-1}. This has been identified as an electric dipole transition from the ground $^7F_6$ Γ_2 state to the $^7F_0$ Γ_1 state as shown in Table VII.

Two lines were observed in the fluorescence data in the wavelength range where one might expect transitions from the $^5D_4$ multiplet. The line at 14 695 cm^{-1} is 21 cm^{-1} above the line at 14 674 cm^{-1}, which is consistent with a higher $\Gamma_{3,4}$ level of the $^5D_4$ multiplet fluorescing to the $^7F_4$ multiplet. The π line is a very small bump, however, and should not be taken very seriously. The σ line is more intense, and is compatible with the absorption data.

8. Other States

A search in the visible wavelength range by absorption measurements to establish the $^5D_3$ and $^5D_4$ energy levels yielded the energy levels shown in Table VIII.

TABLE VI. Energy levels of $^7F_1$ multiplet of Tb^{3+} in $CaWO_4$. The fluorescence data described in columns A, B, and C are used to establish the $^7F_1$ energy levels shown in column D. Columns F and G represent the experimental and theoretical energy levels used to obtain a best set of crystal-field parameters.

No.	A	B	C	D	E	F	G
	$^5D_4$ to $^7F_1$ Γ_x	Description[a]	Energy (cm^{-1})	20 547 cm^{-1} − C (cm^{-1})	Absorption levels (cm^{-1})	Experimental levels (cm^{-1})	Theoretical levels (cm^{-1})
1	Γ_1	Slσ	14 975	5572	5585	5585	5479.3
2	$\Gamma_{3,4}$	bπ	14 852	5695	5702	5702	5586.8

[a] Notation in column B, see Table I.

[11] R. R. Stephens and D. E. Wortman, Harry Diamond Laboratory Report No. TR-1367, 1967 (unpublished).

TABLE VII. Energy levels of $^7F_0$ multiplet of Tb^{3+} in $CaWO_4$. The fluorescence data described in columns A, B, and C are used to establish the $^7F_0$ energy levels shown in column D. Column E gives the $^7F_0$ energy levels established by absorption measurements. Columns F and G represent the experimental and theoretical energy levels used to obtain a best set of crystal-field parameters.

No.	A	B	C	D	E	F	G
	$^5D_4$ to $^7F_0$ Γ_x	Description[a]	Energy (cm^{-1})	20 547 cm^{-1} − C (cm^{-1})	Absorption levels (cm^{-1})	Experimental levels (cm^{-1})	Theoretical levels (cm^{-1})
1	No. 2+21 cm^{-1}	$b\pi$	14 695				
2	Γ_1	$Sl\sigma$	14 674	5873	5890	5890	5709.0

[a] Notation in column B, see Table I.

Three Γ_1 lines of the $^5D_4$ multiplet were established using the electric dipole selection rules and S_4 multiplication tables. A $\Gamma_{3,4}$ level near the lower Γ_1 line could not be ruled out. The lowest-energy $^7F_6$ Γ_2 to $^5D_4$ Γ_1 transition could show up in the σ spectrum if the crystal were not properly aligned. However, such a $\Gamma_{3,4}$ level seemed to be fluorescing to many of the ^7F states corroborating the identification of two very close energy levels, the Γ_1 and $\Gamma_{3,4}$. Other possible levels in the $^5D_4$ multiplet that were not established by the absorption data seemed to be fluorescing also; i.e., a Γ_2 level 50 cm^{-1} above, and a $\Gamma_{3,4}$ level 22 cm^{-1} above the lowest Γ_1 and $\Gamma_{3,4}$ energy levels in the $^5D_4$ multiplet. The levels observed in the region where one might expect transitions from the ground state to the $^5D_3$ and $^5D_4$ multiplets (and some higher states) are listed in Table VIII.

The 37 energy levels identified as discussed above for the ground ^7F term that is listed in column F of Tables I–VII, were used to determine the crystal-field parameters for Tb^{3+} in $CaWO_4$ as described in Sec. IV B.

B. Calculated Results

The best-fit theoretical levels determined for case 3 are listed in column G of Tables I–VII. Figures 1 and 2 are plots of the theoretical energy levels obtained for cases 1, 2, and 3 and of the experimental energy levels. In fitting the theoretical levels to the experimental ones for case 3, the parameters that were varied in the homing-in procedure were η of Eq. (11) and the B_{lm}. The best-fit value for η is 0.64242, from which $\lambda_1(\eta)$ and $\lambda_2(\eta)$ were determined. These parameters, along with the B_{lm} and spin-orbit parameters for all the cases, are listed in Table IX. In Table X the deviation between the theoretical and experimental energy levels for all five cases are evaluated by three different criteria; and the $g_{||}$ factor for the ground state calculated by each case is compared with the experimental value.[6]

In determining what affects the B_{lm}, it was found that the uncertainties in the experimental measurements seem to average out and do not change the B_{lm} appreciably. For example, the center positions of the experimental lines are not known exactly owing to the 10–50-cm^{-1} widths of the lines. When average values for the B_{lm} are determined by computing B_{lm} for many different possible values for the lines, the results are essentially those determined[10] by using just the energies corresponding to the peaks of the lines. In addition, the B_{lm} were found to be somewhat insensitive to the ambiguities that existed concerning the identity of some of the lines; such ambiguities were a result of transitions to both the Γ_2 and $\Gamma_{3,4}$ levels being observed both in the σ and π fluorescence spectra. A consistency check was also made by assigning other symmetry properties to the experimental levels given in Tables I–VII, and each time this yielded a larger rms deviation between the theoretical and experimental levels. The B_{lm} are more sensitive, therefore, to the choice of the theoretical model than to the experimental uncertainties in this work. The degree of sensitivity in the B_{lm} can be seen in Table IX by comparing the results of the five theoretical models.

Line one of Table X shows how well each theoretical model predicts the energy splittings for each J multiplet. This calculation is made by normalizing the theoretical energy centers of gravity for each J multiplet to the experimental energy centers; this is the only fit that is meaningful for case 1. Such a comparison shows that cases 3, 4, and 5 yield a better representation of the observed splittings than do cases 1 and 2. This fact indicates that J mixing and term mixing significantly affect the energy splittings.

TABLE VIII. Absorption lines corresponding to energy range of transitions from ground state to $^5D_3$ and $^5D_4$ multiplets of Tb^{3+} in $CaWO_4$. These lines were observed using 1.50 at.% Tb^{3+} in single crystal of $CaWO_4$. A 1% Tb^{3+} in $CaWO_4$, similarly compensated with Na, yielded several additional small lines.

Transition observed in energy region	π polarization (cm^{-1})	σ polarization and axial spectrum (cm^{-1})
$^7F_6$ to $^5D_3$	27 027	26 969
	27 001	26 896
	26 908	26 589
	26 525	26 511
	26 469	26 434
	26 307	26 378
		26 357
		26 302
		26 288
$^7F_6$ to $^5D_4$	20 637	
	20 552	
	20 542	20 545

TABLE IX. Comparison of crystal-field parameters and spin-orbit parameters for Tb^{3+} in $CaWO_4$ predicted by cases 1–5. These parameters yielded a least-squares fit between the theoretical and experimental energy levels for the ground term where the goodness-of-fit quantities are listed in Table X. The Hamiltonians for the five cases are: (1) $H=H_x=\Sigma_{lm}B^+_{lm}C_{lm}$, (2) $H=\lambda(\mathbf{L}\cdot\mathbf{S})+H_x$, (3) $H=\lambda_1(\mathbf{L}\cdot\mathbf{S})+\lambda_2(\lambda_1)(\mathbf{L}\cdot\mathbf{S})^2+H_x$, (4) $H=\lambda_1(\mathbf{L}\cdot\mathbf{S})+\lambda_2(\mathbf{L}\cdot\mathbf{S})^2+H_x$, (5) $H=\lambda_1(\mathbf{L}\cdot\mathbf{S})+\lambda_2(\mathbf{L}\cdot\mathbf{S})^2+\lambda_3(\mathbf{L}\cdot\mathbf{S})^3+H_x$.

	Case 1	Case 2	Case 3	Case 4	Case 5
B_{20}	446.7	486.1	466.1	466.4	467.8
B_{40}	−882.2	−1092.4	−931.4	−895.3	−825.0
B_{44}	821.7	869.3	1032.4	970.2	872.2
B_{60}	−284.0	−765.8	−182.6	−252.9	−290.5
$\mathrm{Re}B_{64}$	1091.2	480.0	571.6	533.4	595.3
$\mathrm{Im}B_{64}$	≡0.0	0.22	0.023	0.08	159.6
λ (or λ_1)		−271.2	−272.7	−273.5	−254.9
λ_2			−4.837	−4.063	−4.536
λ_3					−0.2413

Line 2 of Table X shows how the rms deviations compare for cases 2–5 when the energy levels are calculated directly, and no manual shifting of the J energy centers is made. Case 2 neglects term mixing, and thus does not account for deviations from the Landé interval rule.[2] Case 3, while containing no more parameters than case 2, nevertheless includes term mixing to second order in the spin-orbit interaction, and as a result gives an rms fit of 60 cm^{-1} compared with 167 cm^{-1} for case 2. Cases 4 and 5 include the higher-order spin-orbit effects in a phenomenological way through the introduction of additional parameters and give rms fits of 52 and 22 cm^{-1}, respectively. These results show that term mixing should be included in the calculations, otherwise the B_{lm} are forced to correct for inadequacies in the free-ion description. The fact that both cases 4 and 5 yield a smaller rms deviation between the theoretical energy levels and the experimental energy levels than case 3 is not surprising, since more free parameters are used in the fit. What should be mentioned is that case 4 shows how a change in the spin-orbit parameters, which might be because of different values for F_2, a, or b, might affect the B_{lm} of case 3, where fixed theoretical values of F_2, a, and b given by Eq. (14) were used. Case 5, which is likewise in the form suggested by Karayianis,[1] indicates how higher spin-orbit terms can affect the B_{lm}. Preliminary work using an effective Hamiltonian, which is to third order in the spin-orbit interaction and exact in the crystal-field interaction, yields values for the B_{lm} in agreement with those of case 5. Such a Hamiltonian (in the form of case 5 but with λ_1, λ_2, and λ_3 coupled by η and F_2) yields spin-orbit parameters in agreement to within 5% of those given in Table IX for case 5. In this latter work,[1] a value of $F_2=419$ cm^{-1} was used rather than 434 cm^{-1} as given by Ofelt.[6] Such a value was obtained by interpolating from an F_2 versus atomic number plot for the triply ionized rare-earth ions.

Line three of Table X gives a summary of the mean error between the theoretical and experimental levels; the mean error allows a better comparison between the various models since the number of free parameters used for each case is not constant. Cases 4 and 5 again yield smaller mean errors, as well as rms deviations between the theoretical and experimental energy levels, than case 3; however, it should be mentioned that case 3 is the most useful in the event that certain multiplets are not observed. For example, when only the absorption data for Tb^{3+} in $CaWO_4$ were available, the $^7F_4$ and $^7F_5$ multiplets were not observed. Then case 3 still yields a good fit to the observed levels and predicts accurately the positions of the missing levels. Case 4 or 5 will again yield a better fit to the measured levels (i.e., to the 16 levels observed in absorption, say) but

TABLE X. Comparison of five Hamiltonians used in fitting ground term of Tb^{3+} in $CaWO_4$. g_{expt} (parallel) $=17.777\pm0.005$; p=No. of free parameters; n=No. of E levels used in fit; $Q^2=\Sigma_i(E_{expt}-E_{theo})_i^2$; rms$=(Q^2/n)^{1/2}$; mean error$=[Q^2/(n-p)]^{1/2}$.

	Case 1	Case 2	Case 3	Case 4	Case 5
Theoretical-experimental rms deviation of E levels after matching E centers of gravity for each J multiplet in cm^{-1}	31.9	24.3	18.0	14.6	12.3
Theor-expt rms deviation of E-levels in cm^{-1}		167.4	60.2	51.8	21.8
Theor-expt mean error for fit of E-levels in cm^{-1}		185.9	66.9	58.5	25.0
g_{theo} (parallel) of ground state	17.996	17.952	17.915	17.927	17.959
No. of free parameters	11	7	7	8	9

will not describe properly the entire ground term. That is, cases 4 and 5 will not predict accurately the positions of the missing multiplets. For this reason the Hamiltonian of case 3 may be more useful in certain cases, but in any event the use of a Hamiltonian derived from fundamental considerations is generally (but not necessarily) to be preferred over phenomenological Hamiltonians. Hence, case 3 was chosen as the standard model to which the other models were compared.

It is useful to compare how well the spin-orbit and B_{lm} might describe other physical phenomena in addition to the energy levels. The parallel component of a g factor, $g_{||}$, for the ground Γ_2 state was calculated for each case. Table X shows that $g_{||}$ of case 3 is 17.915 and is in agreement to about 0.8% with the $g_{||}$ measured in a previous EPR study,[6] yielding $g_{||}=17.777\pm 0.005$. The $g_{||}$ factors, determined using the other Hamiltonians of cases 1, 2, 4, and 5 do not agree as well, but are still within about 1.2% of the measured value.

In summary, the parameters for case 3 as given in Table IX yield theoretical energy levels compatible with the experimental energy levels for the ground term of Tb^{3+} in $CaWO_4$. These parameters also yield results consistent with the $g_{||}$-factor measurement of the ground state. A comparison of the various theoretical models shows that the B_{lm} are affected considerably when J mixing and term mixing are neglected, as they are in cases 1 and 2. Such effects are considered by the effective Hamiltonian (case 3) and the range over which the B_{lm} may vary is indicated by the results obtained for cases 4 and 5.

ACKNOWLEDGMENTS

The author would like to thank Dr. N. Karayianis and Dr. J. Nemarich for many stimulating discussions concerning this work. N. Karayianis is also thanked for the use of some of his computer subroutines and some of his results, which are to be published, concerning Tb^{3+}. Lynwood Randolph is thanked for his help in recording the fluorescence data. The crystals were kindly furnished by W. Viehmann and x-ray-oriented by A. Edwards.

PHYSICAL REVIEW VOLUME 175, NUMBER 2 10 NOVEMBER 1968

Measurement of the Nuclear Spin Diffusion Coefficient in CaF_2†

G. W. LEPPELMEIER* AND J. JEENER
Université Libre de Bruxelles, Bruxelles, Belgium

(Received 17 May 1968)

Measurements are reported of the spin-lattice relaxation time T_1 at 80°K and at room temperature for F^{19} spins in CaF_2 doped with one U^{3+} ion per 9×10^3 fluorine atoms. T_1 was found to be strongly dependent on the orientation of magnetic field with respect to the crystalline axes. Observation at 80°K of the recovery of nuclear magnetization for very short times after saturation indicated a $t^{1/2}$ behavior, as predicted by Blumberg for the diffusion-limited regime of relaxation via paramagnetic impurities. The magnetization which starts out proportional to $t^{1/2}$ consists of spins near a paramagnetic impurity, i.e., those relaxed by direct contact with the paramagnetic ions rather than by diffusion of Zeeman energy via the nuclear dipole-dipole interaction. The latter measurements, coupled with the T_1 measurements, yield values for the effective spin-diffusion coefficient of 0.77×10^{-12} cm²/sec when the dc magnetic field is in the [111] direction, and 4.2×10^{-12} cm²/sec when it is in the [100] direction. These results are in disagreement with present theories, which predict little variation in the effective diffusion coefficient with orientation of the applied field.

INTRODUCTION

WORK in recent years has underlined the importance of transport of nuclear Zeeman energy in solids by the dipole-dipole interactions among nuclear spins, a process usually referred to as nuclear spin diffusion. We wish to report here some experimental results which, while confirming the approximate magnitude of theoretical predictions of the effective spin-diffusion coefficient, disagree strongly with the theoretical prediction of the effect of magnetic field orientation on the diffusion coefficient.

Nuclear spin diffusion is an important phenomenon in the domain of solid-state physics, as is illustrated by at least three examples: The first is as a mechanism enhancing spin-lattice relaxation by paramagnetic impurities. In many insulators the main coupling of the nuclear spins to the lattice is via the electron spins of the paramagnetic impurities. The rate for relaxation of a single nuclear spin by an electron spin is Cr^{-6}, where C is a function of the two magnetic moments, the angle between the applied magnetic field and the line joining the two spins, the correlation time of the electron spin states, and the Larmor frequency of the nuclear spins,[1] and r is the distance between the nuclear spin

* NATO Postdoctoral Fellow. Present address: Lawrence Radiation Laboratory, Livermore, Calif.

† Supported in part by the Fonds National de la Recherche Scientifique and the Instituts Solvay.

[1] N. Bloembergen, Physica **15**, 386 (1949).